J. Membrane Biol. 176, 223–236 (2000)
DOI: 10.1007/s00232001092

The Journal of
Membrane
Biology

© Springer-Verlag New York Inc. 2000

# Mechanisms of Action of Rabbit CAP18 on Monolayers and Liposomes Made from Endotoxins or Phospholipids

**T. Gutsmann[1], M. Fix[2], J.W. Larrick[3], A. Wiese[1]**

[1]Research Center Borstel, Center for Medicine and Biosciences, Department of Immunochemistry and Biochemical Microbiology, Parkallee 10, D-23845 Borstel, Germany

[2]Westfälische Wilhelms-Universität Münster, Institut für Biochemie, Wilhelm-Klemm-Str. 2, D-48149 Münster, Germany

[3]Palo Alto Institute of Molecular Medicine, 2462 Wyandotte Street, Mountain View, California 94043, USA

Received: 14 January 2000/Revised: 20 April 2000

**Abstract.** We have investigated the mechanism of action of the cationic antimicrobial protein (18 kDa) CAP18 on liposomes and monolayers made from phospholipids and enterobacterial lipopolysaccharides (LPS). CAP18 intercalates into lipid matrices composed of LPS from sensitive strains, weaker into those made of LPS from a resistant strain (*Proteus mirabilis* strain R45) or negatively charged phospholipids, but not into those composed of neutral phosphatidylcholine. From the combination of data obtained with fluorescence resonance energy transfer and Fourier-transform infrared spectroscopy and film balance measurements, it can be concluded that structural differences in the LPS determine the depth of intercalation of CAP18 into the respective lipid matrices. Thus, we identified the L-Ara*p*4N linked to the first Kdo of the LPS of *P. mirabilis* strain R45 to be responsible for the CAP18 resistance of this strain. These data provide insight into CAP18-mediated effects on the integrity of the outer membrane of Gram-negative bacteria and led to an improved model for rabbit CAP18 membrane interaction.

**Key words:** CAP18—Monolayer—Liposomes—Outer membrane—Lipopolysaccharide—Resistance

## Introduction

Lipopolysaccharide (LPS, endotoxin) is a potent inducer of Gram-negative sepsis. LPS represents the major amphiphilic surface component of Gram-negative bacteria comprising the lipid matrix of the outer leaflet of the outer membrane, whereas the inner leaflet is composed of a phospholipid (PL) mixture. Chemically, LPS consists of an oligo- or polysaccharide portion covalently linked to a lipid component, termed lipid A, that anchors the molecule in the membrane (Rietschel et al., 1994). The negative molecular charge of the LPS, e.g., the number of carboxyl or phosphoryl groups depends upon the bacterial species and/or strain.

Endogeneous antimicrobial peptides are the front line of host defense against invading microorganisms by direct physicochemical attack on the surface membranes of these foreign pathogens. Being positively charged, these proteins are perfectly suited to interact with negatively charged membranes to cause disruptive changes in membrane permeability. Among these peptides/proteins is the cationic antibacterial protein of 18 kDa (CAP18), which was originally isolated from rabbit granulocytes (Larrick et al., 1991). CAP18 is stored in the intracellular granules of neutrophilic granulocytes and is liberated into the phagocytic vacuoles during phagocytosis (Cowland, Johansen & Borregaard, 1995). The mechanism of action of CAP18 on Gram-negative bacteria has not fully been elucidated. CAP18 exhibits LPS-binding, LPS-neutralizing, antibacterial, and anticoagulant activities and consists of 142 amino acids with the bioactivity found in the C-terminal fragment of 37 amino acids ($CAP18_{106–142}$) (Hirata et al., 1995). This C-terminal fragment carries two negative and 15 positive amino acids and has a high-affinity binding site for heparin (Hirata et al., 1994). Gram-negative bacteria, such as *Escherichia coli*, *Salmonella minnesota* and *Salmonella typhimurium* and Gram-positive bacteria, such as *Streptococcus pneumoniae* and *Staphylococcus aureus* are known to be sensitive towards the antimicrobial action of CAP18 with 50% inhibitory concentrations of 20 to 100

*Correspondence to:* A. Wiese

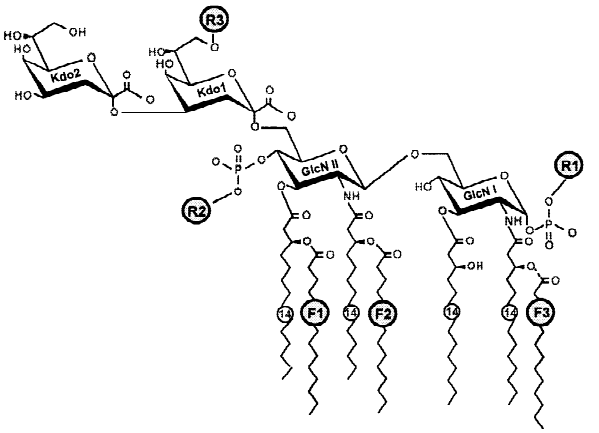


| | F515 LPS | R595 LPS | R45 LPS |
|---|---|---|---|
| R1 | H | H ≥ 90%<br>P-Etn ≤ 10% | H |
| R2 | H | L-Arap4N 65%<br>H 35% | H 50%<br>L-Arap4N 50% |
| R3 | H | H | H 50%<br>L-Arap4N 50% |
| F1 | 14:0 | 14:0 | 14:0 |
| F2 | 12:0 | 12:0 | 14:0 |
| F3 | H | H 70%<br>16:0 30% | H |

**Fig. 1.** Chemical structures of the deep rough mutant lipopolysaccharides used in this study.

nM (0.4 to 2 μg/mL) and 130 to 200 nM (2.3 to 3.6 μg/mL), respectively. There is, however, no activity of CAP18 against the Gram-negative strain *Proteus mirabilis*, against fungi and multiple-drug-resistant strains of *Mycobacterium avium* and *Mycobacterium tuberculosis* (Larrick et al., 1993). A dependence of $CAP18_{106–137}$ activity on the salt concentration of $K^+$ (50 to 250 mM) and $Mg^{2+}$ (1 to 10 mM) was not observed (Mason et al., 1997). The important biological role of human CAP18 in innate immunity was corroborated by Bals et al. (1999) who showed that the transfer of the hCAP18 gene into tracheal epithelium restores bacterial killing in a cystic fibrosis xenograft model.

Many polycationic peptides/proteins, e.g., polymyxin B or defensins, initially cause damage to the outer membrane of Gram-negative bacteria and can reach the cytoplasmic membrane by a "self promoted" uptake (Hancock, 1984; Viljanen, Koski & Vaara, 1988).

Utilizing electrophysiological measurements on planar reconstituted asymmetric lipopolysaccharide/phospholipid bilayer membranes, we recently showed that the mechanism of interaction of CAP18 with these membranes comprises several steps (Gutsmann et al., 1999): After the accumulation of the proteins at the membrane surface and intercalation into the membrane, the orientation of the proteins changes under the influence of an LPS specific clamp-voltage from a nonconductive to a conductive transmembrane state. CAP18 oligo- or multimers then form transient lesions with heterogeneous characteristics and limited lifetimes. We proposed that the CAP18 molecules intercalate into the outer membrane of different strains to different depths and that, therefore, different minimal clamp voltages are required for the induction of membrane lesions. This model could explain the discrimination between sensitive and resistant strains.

In this paper we present results from investigations into the action of rabbit CAP18 on liposomes and monolayers composed of LPS from various sensitive and resistant strains and of negatively charged and neutral phospholipids. We applied different biophysical techniques including fluorescence energy transfer (FRET) spectroscopy on liposomes, monolayer measurements on a Langmuir trough, and Fourier-transform infrared spectroscopy to obtain information on the intercalation of CAP18 into mono- and bilayers, on the influence of mono- and divalent cations, and on the interaction of the protein with various functional groups of LPS and, *vice versa*, the influence of LPS on the conformation of CAP18. LPS with the shortest sugar moieties, i.e., the LPS from deep rough mutant strains (Re LPS) carrying only two 2-keto-3-deoxyoctonate (Kdo) units at the lipid A, was used. A combination of these results with those from our earlier investigations using asymmetric planar bilayers, allow us now to describe the single steps of the proposed multi-step interaction model in more detail. In particular we can understand the mechanisms which lead to a reduced efficacy of the action of CAP18 on resistant Gram-negative strains.

## Materials and Methods

### Lipids and Other Chemicals

For the formation of monolayers and liposomes, deep rough mutant LPS from *Escherichia coli* strain F515 (F515 LPS), *Salmonella enterica* sv. Minnesota strain R595 (R595 LPS), and from *Proteus mirabilis* strain R45 (R45 LPS) (chemical structures according to Zähringer et al., 1985; Rietschel et al., 1992; Rietschel et al., 1994; Vinogradov et al., 1994; Wiese et al., 1998) were used (*see* Fig. 1). LPS was extracted by the phenol/chloroform/petroleum ether method (Galanos, Lüderitz & Westphal, 1969), purified, lyophilized, and transformed into the triethylamine salt form. The amounts of nonstoichiometric substitutions by fatty acids, L-Arap4N, and phosphoethanolamine (P-Etn) were analyzed by MALDI-TOF mass spectrometry. Thus, in the R595 LPS, the 16:0 fatty acid linked to the amide-linked 3-OH-14:0 in position 2 of the reducing glucosamine was present only at a level of 30% and L-Arap4N linked to the 4′-phosphate at a level of 65%. In R45 LPS, approximately 50% of the phosphates linked to the 4′-

**Table 1.** Electrostatic characteristics of Re LPS molecules and Re LPS monolayers in the absence and presence of CAP18

| LPS | Molec. charge[a] $e_0$ | Charge density[a] $e_0/nm^2$ | Surface potential without CAP18 mV | Surface potential with CAP18 mV | Rel. change of potential[b] $\Delta\Phi$ |
|---|---|---|---|---|---|
| F515 LPS | −4 | −3.1 | 350 ± 15 | 470 ± 15 | Decrease |
| R595 LPS | −3.4 | −2.4 | 345 ± 25 | 460 ± 25 | Decrease |
| R45 LPS | −3 | −2.0 | 310 ± 12 | 445 ± 12 | Increase |

[a] Taken from Wiese et al. (1998).
[b] Taken from Gutsmann et al. (1999).
Molecular parameters of the Re LPS monolayers and the surface potential before and after addition of 22 nM CAP18 into the subphase (100 mM KCl, 5 mM $MgCl_2$, 5 mM HEPES, pH 7.0, T = 20°C) at a lateral pressure of 25 $mN \cdot m^{-1}$. The change of the innermembrane potential difference $\Delta\Phi$ after CAP18 addition refers to experiments with asymmetric planar bilayers as published earlier [11]. CAP18 was added to the LPS side of the membranes.

phosphate of lipid A and 50% of the first Kdo were substituted with L-Ara*p*4N. Molecular details of the Re LPS used are listed in Table 1. Lipid A was obtained from F515 LPS by sodium acetate buffer treatment (0.1 M, pH 4.4, 100°C for 1 hr), purified, and converted to the triethylamine salt.

Egg phosphatidylcholine (PC) and phosphatidylglycerol (PG, sodium salt) from egg yolk lecithin were from Avanti Polar Lipids (Alabaster, AL). The phospholipids were used without further purification. The fluorescent dyes N-(7-nitro-2,1,3-benzoxadiazol-4-yl)-PE (NBD-PE) and N-(rhodamine B sulfonyl)-PE (Rh-PE) were purchased from Molecular Probes (Eugene, OR).

Polymyxin B (PMB) was purchased from Sigma (Deisenhofen, Germany). Synthetic rabbit CAP18 was prepared by Merrifield synthesis as previously described (Larrick et al., 1994) and stored in 0.01% acetic acid.

## Resonance Energy Transfer Spectroscopy

The fluorescence resonance energy transfer (FRET) technique was used as a probe dilution assay (Struck, Hoekstra & Pagano, 1981) to obtain information on the intercalation of CAP18 into liposomes made from various phospholipids and lipopolysaccharides. For the FRET measurements, PC, PG, or LPS liposomes were double-labeled with NBD-PE and Rh-PE. The fluorescent dyes were dissolved together with PC, PG, or LPS in chloroform in molar ratios [lipid]:[NBD-PE]:[Rh-PE] of 100:1:1. The solvent was evaporated under a stream of nitrogen, the lipids resuspended in bathing solutions with different salt concentrations at pH 7.0, mixed thoroughly, and sonicated with a Branson sonicator for 1 min (1 ml solution). Subsequently, the preparation was cooled for 30 min at 4°C, heated for 30 min at 56°C, and recooled to 4°C. Preparations were stored at 4°C overnight prior to measurement. A preparation of 900 μl of the double-labeled lipid- or LPS liposomes (0.1 mM) at 37°C was excited at 470 nm (excitation wavelength of NBD-PE), and the intensities of the emission light of the donor NBD-PE (531 nm) and acceptor Rh-PE (593 nm) were measured simultaneously on the fluorescence spectrometer SPEX F1T11 (SPEX, Edison, NY). The protein was added after 50 sec to a final concentration of 2.5 μM. Intercalation could be detected as changes in fluorescence intensities as a function of time (increase of the donor signal, decrease of acceptor signal; for the sake of clarity, in the Results only the donor signal is plotted). To obtain identical intensities before the addition of CAP18, the emissions were recorded for 50 sec under continuous stirring to determine the base line, and the signals of the two channels for registration of the emissions were adjusted to 200,000 cps. To exclude different fluorescence behavior of the dyes in the phospholipid- and LPS-liposomes, i.e., that the intercalation of identical amounts of unlabeled molecules would lead to different changes in the fluorescence intensities, the two systems were calibrated in order to obtain quantitative information on CAP18 intercalation. To guarantee that the unlabeled molecules are actually intercalated in the labeled liposomes, they had to be mixed during liposome preparation in the chloroformic phase. This step requires chloroform solubility of the molecules used for calibration and thus excludes CAP18. Therefore, the phospholipids PC and PE were used instead. The admixture of identical amounts of each of these phospholipids to the labeled phospholipid- and LPS liposomes, respectively, led to changes in fluorescence intensity, which were comparable for PC and PE, but differed for the two liposome systems. Therefore, to get comparable results for CAP18 intercalation into the different lipid matrices, the quotient of the fluorescence intensities (corrected by the dilution effect) and the slope of the intensity changes achieved with liposomes containing unlabeled PC or PE was taken as a measure.

## Film Balance Measurements

Using a film balance, monolayers prepared at the air/water interface can be compressed, and the lateral pressure in dependence on the surface area can be recorded. From pressure/area curves at a given temperature (isotherms) the area per molecule of the monolayer composing lipid or/and protein can be calculated at a given lateral pressure.

For the determination of the molecular area of the CAP18-molecule its capability to form monolayers when added to an aqueous phase was utilized using a Langmuir film balance equipped with a Wilhelmy system (Munitech, München, Germany). CAP18 was added to the aqueous subphase of 100 mM KCl, 5 mM $MgCl_2$ and 5 mM HEPES at pH 7 and 20°C at various concentrations (10 nM to 20 nM), and the system was allowed to equilibrate for 2 hr. Pressure/area isotherms were than recorded at a compression rate of 1.5 $mm^2 \cdot s^{-1}$. From the different isotherms obtained at the various CAP18 subphase concentrations, the total film area was determined at a lateral pressure of 25 $mN \cdot m^{-1}$. Then, the number of CAP18 molecules added to the subphase was plotted as a function of these values. The molecular area of CAP18 molecules was obtained from the slope of this curve and the amount of protein remaining in the subphase and/or bound to the walls

of the trough was estimated from the intersection of the curve with the *x*-axis (Schwarz & Taylor, 1995).

The incorporation of the protein into lipid monolayers with respect to the composition of the aqueous subphase was studied with monolayers spread from 1 mM chloroform solutions of PC and PG, respectively, and with chloroform/methanol (9:1 v/v) solutions of LPS. The experiments were run at 37°C. Prior to isotherm recording, monolayers were equilibrated at zero pressure for 5 min to allow evaporation of the solvent. The monolayers were then first compressed to a lateral pressure of 30 $mN \cdot m^{-1}$ for 30 min to check the stability of the monolayer and subsequently expanded to 25 $mN \cdot m^{-1}$ [this value is within the range of lateral pressures discussed to prevail in biological bilayer membranes (Marcelja, 1974; Blume, 1979)]. CAP18 was added to the subphase in different concentrations (0 to 25 nM), and the change in film area versus time was plotted for 1 hr. The expansion isotherms were then recorded at an expansion rate of 1.5 $mm^2 \cdot s^{-1}$. To examine the influence of $Mg^{2+}$ ions, compression and expansion isotherms for F515 LPS monolayers after addition of the protein into the subphase were recorded in the absence and presence of 5 and 20 mM $MgCl_2$.

The surface potential was determined with a vibrating plate condenser (KP2, NimaTechnology, Coventry, England) on a film balance (601M, Nima Technology, Coventry, England) as described in several papers (Pickard, Sehgal & Jackson, 1979; Vogel & Möbius, 1988; Schumann, 1989; Brockman, 1994). The procedures of monolayer preparation and addition of CAP18 were as described above. Subphase temperature was chosen as 20°C to avoid condensation of water at the vibrating plate.

For epifluorescence microscopic studies (von Tscharner & McConnell, 1981; Weis, 1991), the fluorescent dye NBD-PE was codissolved with F515 LPS or the lipid A from F515 LPS in chloroform/methanol in molar ratios [lipid]:[NBD-PE] of 100:2. Monolayers were prepared and CAP18 was added as described above. The monolayers were compressed at 45 $mN \cdot m^{-1}$ to increase the number and size of the liquid condensed (LC) domains within the liquid expanded (LE) monolayer which are formed during the pressure-induced LE↔LC phase transition. Using the fluorescent dye NBD-PE — which had no significant influence on the isotherms — the LE domains appeared light and the LC domains dark. The images from the epifluorescence microscope (Modell 1, Munitech, München, Germany) were recorded by a video camera (C2400-08-C, Hamamatsu, Hamamatsu City, Japan) and digitized by a video grabbing-card (Screen Machine II, Fast Electronic, München, Germany).

To investigate the capacity of CAP18 to displace divalent $Ca^{2+}$ ions from LPS monolayers, a subphase containing 12.5 μM $Ca^{2+}$ doped with radioactive $^{45}Ca^{2+}$ (Amersham Buchler, Braunschweig, Germany) and 5 mM HEPES at pH 7 was used. This $Ca^{2+}$ concentration was sufficient for saturating the Re LPS monolayer (160 nM F515 LPS). The low-energy β-radiation of $^{45}Ca^{2+}$ is detected only from a thin surface layer (the radiation from deeper layers is absorbed by the water). Thus, this method allows the determination of the $Ca^{2+}$ concentration in the monolayer (Lüllmann, Plösch & Ziegler, 1980). After spreading the lipid monolayer on the subphase, $Ca^{2+}$ binds to the negatively charged headgroups of the lipids and, therefore, an increase in β-intensity is observed using a β-counter (gas ionization detector LB124, Berthold, Wildbad, Germany). In the displacement experiments it was necessary to keep the number of LPS molecules, and therefore the potential number of binding sites for $Ca^{2+}$, underneath the detection area of the β-counter before and during the intercalation of CAP18 constant. To guarantee this, CAP18 was added to the subphase at a constant area and relatively low lateral pressure of the monolayer (10 $mN \cdot m^{-1}$). This way, the final pressure after saturated intercalation of CAP18 was still in the range of lateral pressures in biological membranes. The peptide was added to the subphase in different concentrations, and the equilibrium β-counting rates were recorded. The relative $^{45}Ca^{2+}$ concentration was calculated by

$$I_{Rel} = \frac{I_{Peptide} - I_{Sub}}{I_{Mono} - I_{Sub}} \quad (1)$$

where $I_{Rel}$ is the relative $^{45}Ca^{2+}$ intensity and $I_{Sub}$, $I_{Mono}$, and $I_{Peptide}$ are the β-intensities of the pure subphase, after spreading the monolayer, and after peptide addition, respectively. The experiments were performed at a subphase temperature of 20°C to avoid condensation at the β-counter.

### FTIR Spectroscopy

This technique was used to obtain information on the influence of CAP18 on the phase behavior and the mobility of the phosphate groups of LPS and, *vice versa*, of LPS on the secondary protein structure of CAP18. For this, all lipid samples were prepared as aqueous suspensions in 10 mM HEPES buffer at pH 7 (20 mM lipid corresponding to appr. 96% water content). The lipids were suspended directly in dist. water and temperature-cycled twice between 4°C and 70°C and then stored at 4°C for at least 12 hr prior to measurement. CAP18 was added in appropriate concentrations and the mixtures were briefly vortexed at 37°C. Measurements were performed on a Bruker FTIR spectrometer IFS55 (Bruker, Karlsruhe, Germany). The lipid samples were placed in a $CaF_2$-cuvette separated by a 12.5 μM thick teflon spacer. Temperature scans were performed automatically in the range from 10°C to 65–80°C at a heating rate of 0.6°C/min. Every 3°C, 50 interferograms were accumulated, apodized, Fourier-transformed, and converted to absorbance spectra.

The evaluation of the band parameters (peak position and intensity) was performed after subtraction of superimposed water bands. Thus, the position of the peak maxima could be determined with a precision of better than 0.1 $cm^{-1}$.

The β↔α gel to liquid crystalline phase transition of the hydrocarbon chains was determined from changes in the peak position of the symmetric stretching vibration of the methylene groups $\nu_s(CH_2)$. It is known to lie at approximately 2850 $cm^{-1}$ in the gel (β) phase and to shift at a lipid-specific temperature, the phase transition temperature $T_c$, to 2852.0–2852.5 $cm^{-1}$ in the liquid crystalline (α) phase (Mantsch & McElhaney, 1991). The interaction of the protein with the lipid headgroups was studied by monitoring the antisymmetric stretching vibration of the negatively charged phosphate groups $\nu_{as}(PO_2^-)$ in the range from 1220 $cm^{-1}$ to 1260 $cm^{-1}$.

For the determination of the protein secondary structure, lipid samples were prepared as described above and the protein was added in different concentrations. Excess water was removed by incubation at 37°C. The secondary structure of CAP18 was determined by analyzing the amide I band contour between 1700 and 1600 $cm^{-1}$, which consists of different intrinsic band components depending on the type of protein conformation (Arrondo et al., 1993). The number of band components and their approximate peak positions were evaluated by Fourier deconvolution (Kauppinen et al., 1981). The single band components were calculated applying a curve-fit procedure (kindly provided by D. Moffat, NRC Ottawa), in which the bands were approximated by combining Lorentzian and Gaussian shapes. Best fits were achieved by taking a Gaussian:Lorentzian ratio of 0.6.

## Result

### Resonance Energy Transfer Spectroscopy

FRET spectroscopy is commonly used to investigate the intercalation of peptides/proteins into lipid membranes

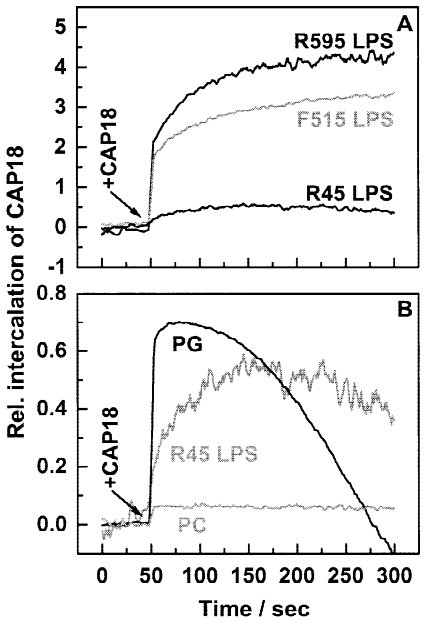


**Fig. 2.** Influence of the lipid matrix on the intercalation of rabbit CAP18 into liposomes. Changes of the normalized donor (NBD-PE) fluorescence intensities in dependence on time after addition of 2.5 μM CAP18 to 100 μM suspensions of liposomes double-labeled with NBD-PE and Rh-PE. Bathing solution: 100 mM KCl, 5 mM $MgCl_2$, 5 mM HEPES at pH 7 and 37°C.

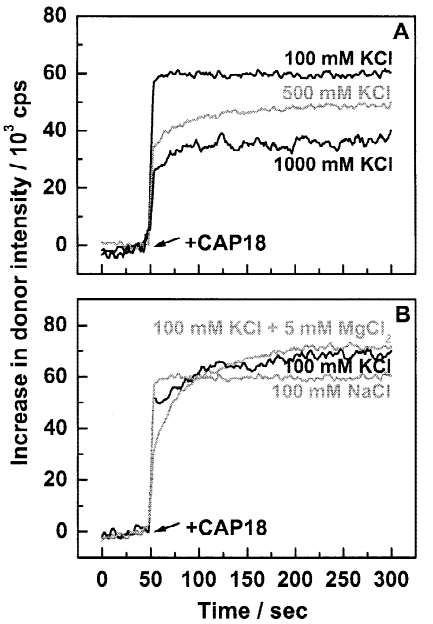


**Fig. 3.** Influence of the salt concentration on the intercalation of CAP18 into F515 LPS liposomes. Changes of the donor (NBD-PE) fluorescence intensities in dependence on time after addition of 2.5 μM CAP18 to 100 μM suspensions of F515 LPS liposomes double-labeled with NBD-PE and Rh-PE. The bathing solution contained the indicated salt concentrations and 5 mM HEPES at pH 7 and 37°C.

by determining the energy transfer between two fluorescent markers (Schromm et al., 1998). The results for CAP18 are shown in Fig. 2. As can be seen from the donor signal after addition of 2.5 μM CAP18 to the 100 μM liposome suspensions, three different groups can be distinguished according to the intensity of interaction between CAP18 and the lipids: F515 LPS and R595 LPS show a strong interaction with CAP18, R45 LPS and PG a weak interaction and there was no intercalation of CAP18 into PC liposomes (Fig. 2). For PG liposomes, the donor signal increased after addition of CAP18, but after 50 sec a decrease was observed caused by precipitation of the liposomes.

The influence of cations on the CAP18 interaction with membranes was investigated using F515 LPS liposomes suspended in different bathing solutions. The changes of the interaction of CAP18 with the lipid matrices were reduced by an increase in the $K^+$ concentration, e.g., at a KCl concentration of 1,000 mM the change in the donor signal was about 40% of that observed at the commonly used 100 mM KCl (Fig. 3*A*). However, at a KCl concentration of 1,000 mM, the change of the donor signal as a consequence of CAP18 addition to F515 LPS liposomes (Fig. 3*A*) was still significantly higher than in the case of R45 LPS liposomes in a 100 mM KCl bathing solution (Fig. 2). No difference in the influences of the monovalent cations $K^+$ and $Na^+$ on the action of CAP18 at cation concentrations up to 1,000 mM was observed as shown for 100 mM in Fig. 3*B*. Also the further addition of 5 mM $Mg^{2+}$ — this concentration was used in most experiments presented in this paper and also in former experiments (Gutsmann et al., 1999) — had no influence (Fig. 3*B*). Higher concentrations of $Mg^{2+}$ led to a fusion of the liposomes thus making a comparison of the changes of the donor signals impossible.

## Film Balance Measurements

When amphiphilic or hydrophobic molecules are added to an aqueous phase (subphase), they tend to adsorb to the air/water interface and, thus, reduce the surface tension of the subphase.

Accordingly, the addition of CAP18 to the subphase of a film balance led to the formation of a protein monolayer at the air/water interface. In Fig. 4*A*, pressure/area isotherms of CAP18 monolayers on subphases containing 100 mM KCl, 5 mM $MgCl_2$, and 5 mM HEPES at 20°C are depicted for different concentrations of CAP18 in the subphase. In Fig. 4*B*, the relation between the number of molecules added to the subphase and the area occupied are plotted for a lateral pressure of 25 $mN \cdot m^{-1}$. From these data, using a regression analysis, the molecular area of one CAP18 molecule at the air/water interface was calculated to be (5.3 ± 0.6) $nm^2$. Correspondingly, these values have been determined in

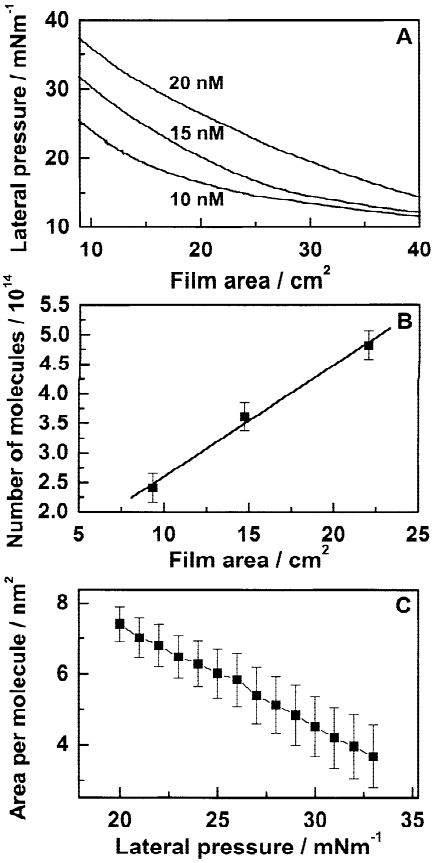


**Fig. 4.** (*A*) Surface-pressure/area isotherms of CAP18 monolayers on CAP18 suspensions of different concentrations. (*B*) Estimation of the molecular area of CAP18 molecules at a lateral pressure of 25 mN · m$^{-1}$. (*C*) Molecular area of CAP18 as a function of the lateral pressure. Bathing solution: 100 mM KCl, 5 mM $MgCl_2$, 5 mM HEPES at pH 7 and 20°C.

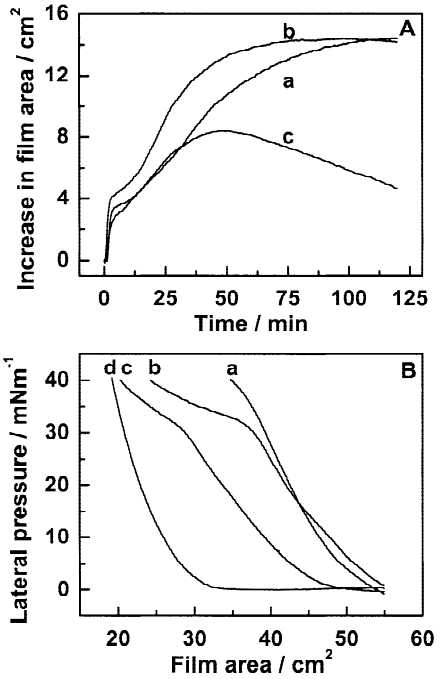


**Fig. 5.** Intercalation of CAP18 into F515 LPS monolayers on different subphases. (*A*) Increase in the film area of F515 LPS monolayers (concentration of the LPS was 3 nmol (75 nM)) after addition of 14 nM CAP18 to the subphase in dependence on time at a constant lateral pressure of 25 mN · m$^{-1}$. (*B*) Compression isotherms of LPS monolayers before (d) and after addition of CAP18 (a, b, c). Bathing solutions: (a) 0 mM $MgCl_2$, (b) 5 mM $MgCl_2$, (c) 20 mM $MgCl_2$ and for all 100 mM KCl, 5 mM HEPES, pH 7, and 37°C.

the lateral pressure range of 20–33 mN · m$^{-1}$, covering the lateral pressure of natural membranes. The area per CAP18 molecule showed an inverse linear correlation to the lateral pressure (Fig. 4*C*).

For LPS (Fig. 5*A*) and PG monolayers (*data not shown*), the addition of CAP18 into the subphase led to an increase in film area at a constant pressure of 25 mN · m$^{-1}$, whereas for a PC monolayer under identical conditions no significant change in film area could be observed (*data not shown*).

To elucidate the influence of divalent cations on the interaction between the cationic CAP18 and the anionic LPS, we investigated the intercalation of CAP18 into F515 LPS monolayers at different $MgCl_2$ concentrations in subphases containing 100 mM KCl and 5 mM HEPES. CAP18 was added to the subphase after the monolayers were compressed to 25 mN · m$^{-1}$, and the time scans of the changes in monolayer area were recorded (Fig. 5*A*). $Mg^{2+}$ concentrations up to 5 mM had little or no influence on the intercalation (Fig. 5*A* traces a, b), however, at a concentration of 20 mM the intercalation was reduced (Fig. 5*A* trace c). Subsequently to the time scan measurements, the monolayers were expanded (0 mN · m$^{-1}$) and compressed to 40 mN · m$^{-1}$. In Fig. 5*B* (traces a, b, c) the respective compression isotherms are shown together with that of the pure LPS monolayer on a $MgCl_2$ free subphase (trace d). As already observed in the time scans (Fig. 5*A*), addition of CAP18 leads to an increase of the area of F515 LPS monolayers, the isotherms are shifted to the right. The shift, however, depends on the $Mg^{2+}$ content of the subphase. At a lateral pressure of 25 mN · m$^{-1}$, the isotherms at 0 mM $Mg^{2+}$ (trace a) and 5 mM $Mg^{2+}$ (trace b) are shifted nearly by identical values, whereas at 20 mM $Mg^{2+}$ this shift is significantly smaller (trace c). At lateral pressures >30 mN · m$^{-1}$, the slope of the isotherms of the CAP18 containing F515 LPS monolayers decreased. This effect was most pronounced in the presence of $Mg^{2+}$ (traces b and c). This indicates a displacement of the already incorporated CAP18 from the monolayers.

The FRET experiments showed a reduced interaction of rabbit CAP18 with R45 LPS as compared to F515 LPS and R595 LPS liposomes (Fig. 2). To clarify, whether this effect results from a reduced binding stoi-

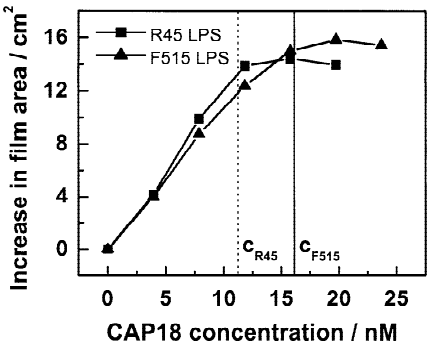


**Fig. 6.** Increase in the film area of F515 LPS and R45 LPS monolayers (concentration of the LPS was 3 nmol (75 nM)) after addition of increasing amount of CAP18 at a lateral pressure of 30 mN · m$^{-1}$. Bathing solution: 100 mM KCl, 5 mM $MgCl_2$, 5 mM HEPES at pH 7 and 37°C.

chiometry or a different orientation of the protein in the membrane, we explored the intercalation of different amounts of CAP18 into F515 LPS and R45 LPS monolayers (concentration of LPS was 3 nmol (75 nM)) at a lateral pressure of 30 mN · m$^{-1}$ on subphases containing 100 mM KCl, 5 mM HEPES and 0 or 5 mM $MgCl_2$, respectively, at pH 7 and 37°C (Fig. 6). The area of one intercalated CAP18 molecule was calculated from the slope of the linear part of the curve in Fig. 6 prior to saturation of the monolayer by CAP18. We considered that a certain amount of the protein remains in the subphase and/or bound to the walls of the trough and does not intercalate into the monolayer. To calculate the binding stoichiometry between CAP18 and LPS, the molar concentration of LPS molecules was divided by the saturation concentration of CAP18 molecules intercalated into the monolayer, which is the difference between the protein concentration in the subphase necessary to obtain saturation in the monolayer (Fig. 6, $c_{R45}$ and $c_{F515}$) and the concentration of the protein remaining in the subphase. The results are summarized in Table 2 showing a reduced binding stoichiometry between CAP18 and F515 LPS or R45 LPS, respectively, in the presence of 5 mM $Mg^{2+}$.

The interactions of cationic peptides/proteins with anionic lipid monolayers may cause displacement of divalent ions such as $Ca^{2+}$ from the monolayers. Monitoring of changes of the $Ca^{2+}$ concentration at the monolayer surface as a consequence of the interaction of polycationic molecules may, thus, provide information on the binding process. To this end, the relative $^{45}Ca^{2+}$ concentration was determined for different concentrations of the peptide in the subphase. For comparison measurements were also performed for polymyxin B (PMB), which is known to bind strongly to negatively charged lipids and to reduce their zeta-potential (Wiese et al., 1997). The influence of the two peptides on the amount of $Ca^{2+}$ bound to 9.6 nmol (160 nM) F515 LPS has been determined from the decrease in relative β-radiation intensity in dependence of peptide concentrations (Fig. 7). In the case of CAP18 47 nM was sufficient to displace 50% of the $Ca^{2+}$ ions, whereas a concentration of 840 nM PMB was needed.

**Table 2.** Size and binding stoichiometry of intercalated CAP18 molecules into F515 LPS or R45 LPS monolayers

| LPS/Subphase | Area per molecule/nm$^2$ | [LPS]:[CAP18] (M/M) |
|---|---|---|
| F515 LPS/Sub.: +0 mM $MgCl_2$ | 3.8 ± 0.5 | 3.5 ± 0.5:1 |
| F515 LPS/Sub.: +5 mM $MgCl_2$ | 3.8 ± 0.6 | 5 ± 0.5:1 |
| R45 LPS/Sub.: +0 mM $MgCl_2$ | 3.8 ± 0.5 | 5 ± 0.5:1 |
| R45 LPS/Sub.: +5 mM $MgCl_2$ | 4.5 ± 0.5 | 6 ± 0.5:1 |

The monolayers were prepared on a subphase containing 100 mM KCl, 5 mM HEPES with varying concentrations of $MgCl_2$ (first column) at pH 7 and a temperature of 37°C. The intercalation was determined at a lateral pressure of 30 mN · m$^{-1}$.

In continuation of earlier work (Gutsmann et al., 1999) we investigated the different influences of CAP18 on the innermembrane potential difference ΔΦ of F515 LPS/PL and R595 LPS/PL bilayers on the one hand and R45 LPS/PL bilayers on the other, by determining the surface potential of monolayers of the respective LPS. As described here for F515 LPS, after compression of the monolayer to 25 mN · m$^{-1}$, a surface potential of (350 ± 15) mV was measured in a subphase containing 100 mM KCl, 5 mM $MgCl_2$, and 5 mM HEPES at pH 7 and 20°C. After addition of 22 nM CAP18 into the subphase, the surface potential remained unchanged for about 30 sec and then increased to a final value of (470 ± 15) mV (Fig. 8*A* and *B*). The time delayed increase in surface potential can be explained by the time necessary for the CAP18 molecules to diffuse to the detection area. After the time scan, the monolayer was expanded, and a slight decrease in the surface potential in dependence on the lateral pressure was observed. For R595 LPS and even for R45 LPS monolayers the same characteristics in the isotherms and time scans were observed (*data not shown*). The values of the surface potentials before and after addition of CAP18 to the different LPS monolayers are given in Table 1.

No effect of the subphase temperature on the intercalation of CAP18 into F515 LPS monolayers was observed in the range of 20–40°C (*data not shown*).

To observe changes in liquid expanded/liquid condensed domain structure of F515 LPS and lipid A monolayers by CAP18, the monolayers were doped with 2% NBD-PE and epifluorescence microscopic studies were performed. At lateral pressures ⩾20 mN · m$^{-1}$, LC domains, appearing dark, were formed in lipid A (3 nmol (75 nM)) monolayers as shown for 40 mN · m$^{-1}$ in Fig. 9*A*. After the addition of CAP18 (4 nM) to the subphase, first the appearance of structurally different areas be-

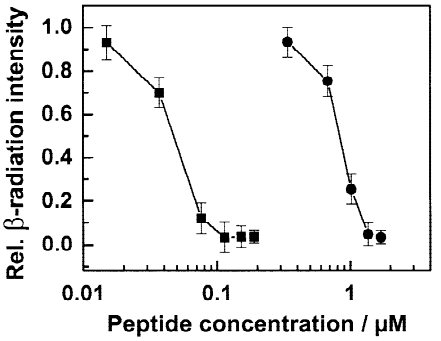


**Fig. 7.** Displacement of $^{45}Ca^{2+}$ from F515 LPS monolayers by polymyxin B and CAP18. Relative change of β-radiation intensity in dependence on peptide/protein concentration after addition of polymyxin B (●) or CAP18 (■). The bathing solution was 12.5 μM total $Ca^{2+}$, 10 mM HEPES at pH 7 and 20°C and the F515 LPS concentration was 9.6 nmol (160 nM).

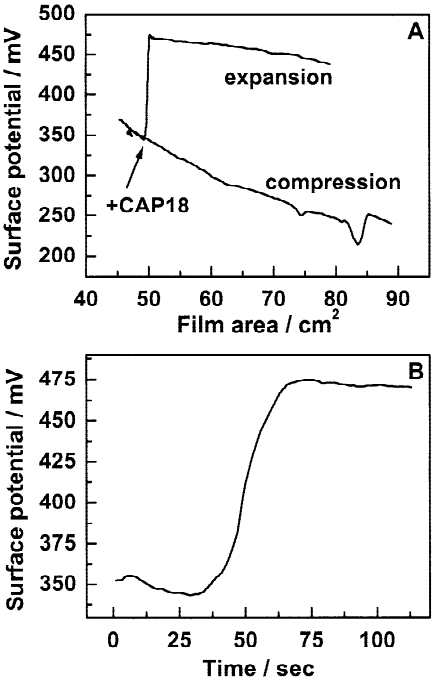


**Fig. 8.** Surface potential of a F515 LPS monolayer (concentration of the LPS was 9 nmol (180 nM)) before and after addition of 22 nM CAP18. (*A*) Surface potential in dependence on film area and (*B*) surface potential in dependence on time after addition of CAP18 at a constant lateral pressure of 25 mN · $m^{-1}$. Bathing solution: 100 mM KCl, 5 mM $MgCl_2$, 5 mM HEPES, pH 7, and 20°C.

tween the LE and LC domains (as can be seen from the grey tone in Fig. 9*B*) and finally a reduction in the LC domains was observed (Fig. 9*C*). Similar effects were observed for Re LPS monolayers (*data not shown*).

## FTIR Spectroscopy

The secondary structure of CAP18 in buffer in the absence and presence of different lipids was determined

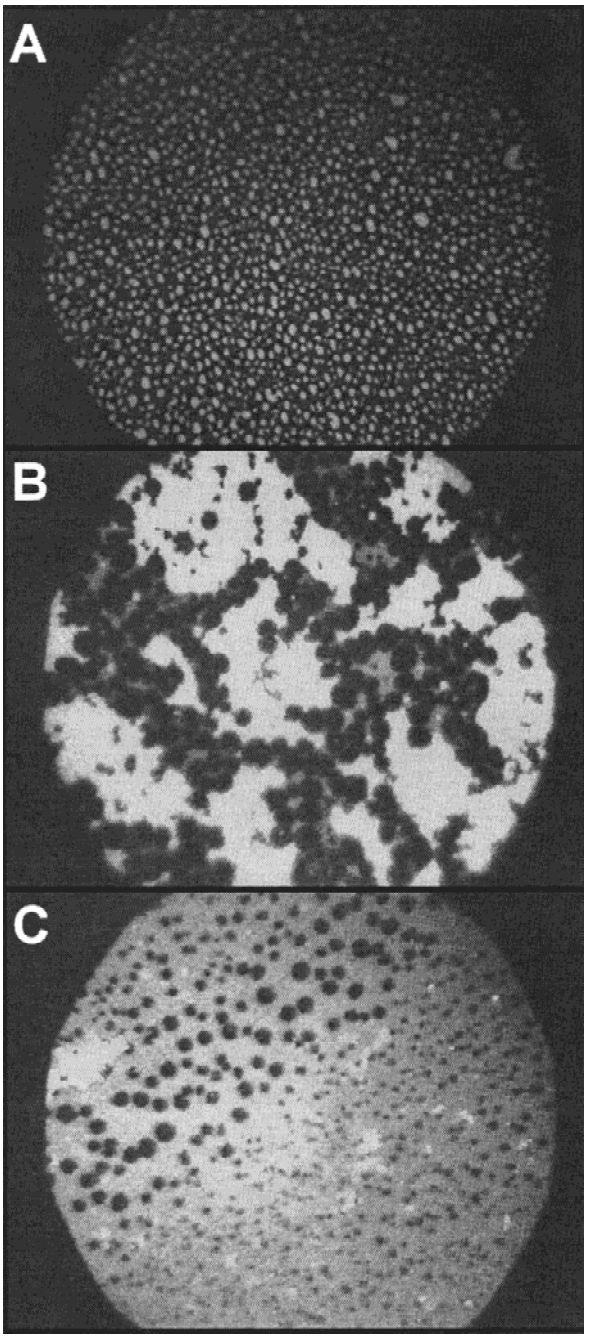


**Fig. 9.** Epifluorescence micrographs of lipid A (from *E. coli*) monolayers labeled with NBD-PE in molar ratios [lipid A]:[NBD-PE] of 100:2 at a lateral pressure of 40 mN · $m^{-1}$. (*A*) Monolayer before CAP18 addition, (*B*) after addition of 4 nM CAP18 at a lateral pressure of 25 mN · $m^{-1}$ and compression to 40 mN · $m^{-1}$ and (*C*) after 30 min. LE domains appear light, LC domains dark. The bathing solution was 100 mM KCl, 5 mM HEPES at pH 7 and 20°C and the total lipid concentration was 3 nmol (75 nM). The diameters of the micrographs are 300 μm.

with infrared spectroscopy by analyzing the amide I band contour in the wavenumber range 1700–1600 $cm^{-1}$. Fourier deconvolution (Kauppinen et al., 1981) and curve fitting (Arrondo, 1993) revealed that this band con-

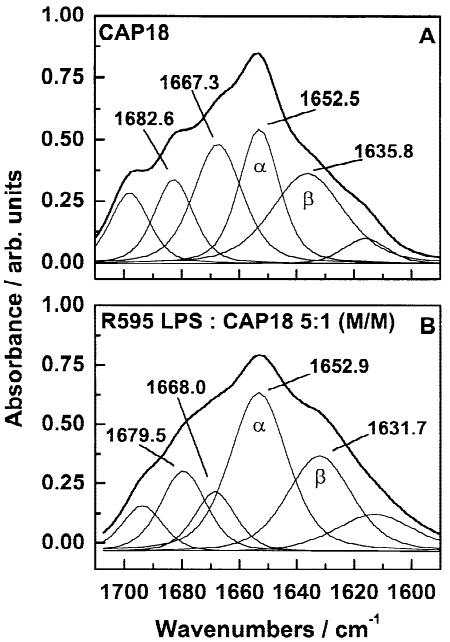


**Fig. 10.** Influence of R595 LPS on the secondary structure of CAP18. Infrared absorbance spectra for CAP18 suspensions in HEPES (10 mM) buffer in the range of the amide I band between 1700 and 1600 $cm^{-1}$ and their band analysis. Spectra of (*A*) pure CAP18 and (*B*) R595 LPS and CAP18 in a molar ratio [lipid]:[CAP18] of 5:1 all at 25°C.

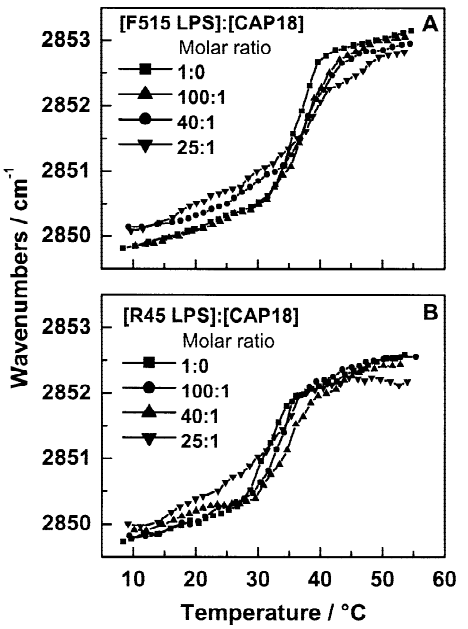


**Fig. 11.** Influence of CAP18 on the phase transition temperature of LPS. Peak position of the symmetric stretching vibrational band $\nu_s(CH_2)$ *vs* temperature for 20 mM (*A*) F515 LPS and (*B*) R45 LPS suspensions in HEPES (10 mM) buffer at different amounts of CAP18.

tour consists of six band components with a characteristic pattern which indicates the occurrence of α-helical and β-sheet structures (Fig. 10*A*). This pattern changed upon the interaction of Re LPS leading to an increase of the band intensities corresponding to α-helices and β-strands indicating an increase in protein overall order. This is shown for CAP18 in the presence of R595 LPS (molar concentration ratio 5:1) in Fig. 10*B.* The increase of α-helical structures was particularly significant also for F515 LPS and R45 LPS, but not for PG (*data not shown*).

CAP18 has only a slight effect on the phase behavior of LPS. The increase of the wavenumber value of the $\nu_s(CH_2)$ band in the gel phase indicates only a slight fluidizing effect below the phase transition temperature $T_c$ of F515 LPS ($T_c \approx 36$°C) and R45 LPS ($T_c \approx 33$°C), the decrease in the liquid crystalline phase is indicative of a slight rigidifying effect (Fig. 11). The protein had no significant influence on $T_c$.

The antisymmetric stretching vibration of the negatively charged phosphate $\nu_{as}(PO_2^-)$ was used as an indicator of an interaction of the polycationic CAP18 with the backbone region of the endotoxins. For Re LPS, it is split into two vibrational bands indicating different hydration states (Fig. 12*A* and *B*; band I, II), with the band at the higher wave number representing a lower hydration (Brandenburg, Kusumoto & Seydel, 1997). Addition of CAP18, which in pure form gives rise to a vibrational band around 1200 $cm^{-1}$ (Fig. 12*A* and *B;* band III), leads to a strong reduction of the band intensities indicating immobilization of the phosphate groups. Interestingly, for R595 LPS the binding of CAP18 leads to a reduction of band I, while for LPS R45 a reduction of band II is more pronounced.

## Discussion

In earlier investigations into the interaction of CAP18 with the reconstituted planar lipid matrix of the outer membrane (Gutsmann et al., 1999), we have observed the formation of transient membrane lesions with short but heterogeneous lifetimes and variable sizes. These characteristics of the lesions were lipid-independent. However, for the induction of the lesions, a lipid-specific clamp-voltage was required. From these findings, we proposed a model for the action of CAP18 which is comprised of the following five steps: (i) accumulation of CAP18 at the membrane surface (aqueous state), (ii) intercalation of the protein into the membrane in a lipid-specific orientation (nonconductive surface state), (iii) change of orientation of the protein by a lipid-specific outside positive clamp-voltage [also required in step (iv)] (nonconductive prelesion state), (iv) formation of transient lesions (conductive state), and (v) closing of lesions (nonconductive postlesion state).

In the present study, we have characterized the interaction of CAP18 with various membrane systems using different biophysical techniques. The aim of the

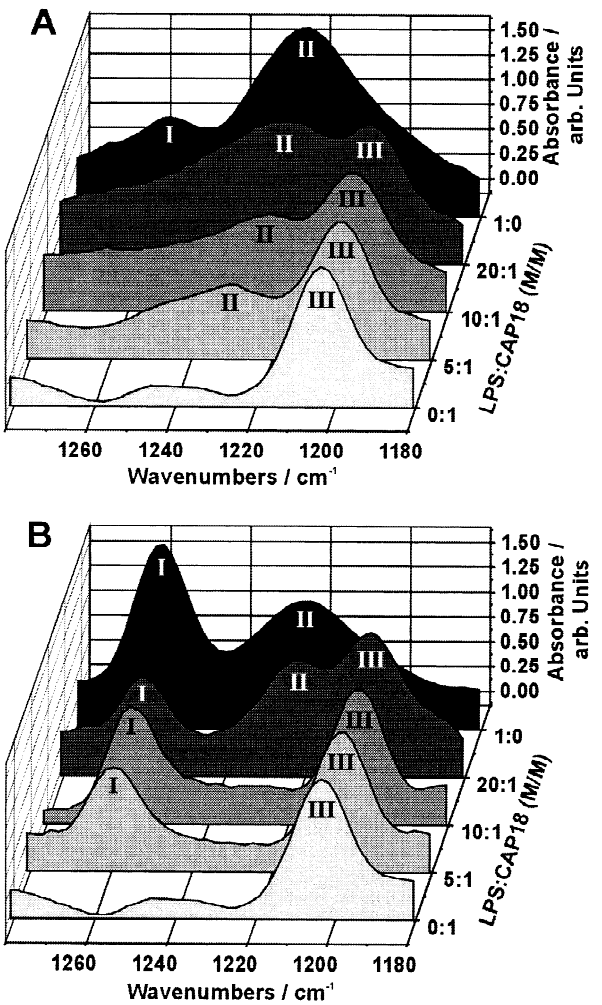


**Fig. 12.** Influence of CAP18 on the headgroups of LPS. Infrared absorbance spectra for (*A*) R595 LPS and (*B*) R45 LPS suspensions in HEPES (10 mM) buffer in the range of the asymmetric stretching vibration of the negatively charged phosphates $\nu_{as}(PO_2^-)$ at 37°C at different molar ratios of CAP18. I, II: vibrational bands of LPS corresponding to different hydration of the phosphates; III: IR band of CAP18.

study was to elucidate in more detail the mechanism of interaction of CAP18 with the outer membrane of Gram-negative bacteria. In particular, the question of CAP18 resistance was investigated comparing the effects on membranes made from LPS from sensitive (F515 LPS and R595 LPS) and resistant (R45 LPS) bacteria.

### Influence of the Type of Lipid Matrix on the Orientation of CAP18 in, or Depth of, its Intercalation into the Bilayers

The interaction of CAP18 with lipid liposomes and monolayers has been studied with FRET spectroscopy and in film balance experiments, which both provided evidence that a negative surface charge is the basic requirement for an intercalation of the protein into lipid matrices, as it was shown for other polycationic antibacterial peptides/proteins such as magainin (Matsuzaki, 1998). Furthermore, from the differences observed for the intercalation of CAP18 into the differently composed monolayers and liposomes from different lipids, information on the mode of intercalation could be derived. The observed fivefold higher increase of the fluorescence intensity of the donor dye after CAP18 addition to liposomes made from R595 LPS and F515 LPS as compared to those from R45 LPS and PG (Fig. 2) could have three reasons: (i) a significantly higher amount of intercalated CAP18, (ii) a different orientation of the protein in the bilayer, or (iii) a different depth of intercalation, which would influence the resonance energy transfer between donor-acceptor pairs in the inner leaflet and between the inner and outer leaflet of the bilayer. These three possibilities can be distinguished on the basis of the data from the monolayer experiments. The molecular area of CAP18 was determined from pure CAP18 monolayers to be (4.5 ± 0.6) $nm^2$ at 30 $mN \cdot m^{-1}$ (Fig. 4*C*). When CAP18 is intercalated into F515 LPS or R45 LPS monolayers, its effective molecular area was only (3.8 ± 0.6) $nm^2$ (Fig. 6, Table 2). This reduction of the effective molecular area could have two reasons: (i) the orientation of CAP18 molecules in LPS matrices differs from that in pure protein monolayers and/or (ii) the mixture of the large CAP18 with the smaller LPS molecules leads to a higher packing density. However, the observed decrease in size cannot only be explained by a higher packing density, because already the size of the fragment $CAP18_{106-142}$ is about 5 nm × 1.8 nm (Chen et al., 1995) which is in the range of the area occupied by the holo protein in the LPS monolayer. Thus, it is unlikely that CAP18 is oriented parallel to the monolayer surface as discussed for magainin 2 (Bechinger, Zasloff & Opella, 1993). Moreover, these film balance experiments showed that the amount and also the molecular area of CAP18 intercalated either into F515 LPS or into R45 LPS monolayers is nearly identical up to saturation (Table 2). In combination with the data from FRET spectroscopy, we conclude that CAP18 intercalation into F515 LPS and R45 LPS matrices occurs almost in the same orientation, but at different depths.

This interpretation is further backed by the observation of changes in the intensity of the vibrational bands of the phosphates of LPS. On the basis of their different degrees of hydration (Fringeli & Günthard, 1981), the two vibrational bands at wavenumber 1260 $cm^{-1}$ (component I) and at wavenumber 1224 $cm^{-1}$ (component II) have previously been shown to originate mainly from the 4′-phosphate and the 1-phosphate, respectively (Brandenburg, Kusumoto & Seydel, 1997). From Fig. 12 it can be seen, that CAP18 has a distinct binding affinity to

the backbone region of both LPS. In the case of R595 LPS the interaction with the less hydrated 4′-phosphate, which is buried in the hydrophobic region, and in the case of R45 LPS with the more hydrated 1-phosphate facing the aqueous phase is more pronounced. The observation of a different influence of CAP18 on the two phosphates of LPS R595 and LPS R45 is, thus, indicative of a deeper intercalation of CAP18 into LPS R595 than into R45 LPS membranes.

The different depth of intercalation into the membrane does also explain the results of the surface potential measurements on lipid monolayers (Fig. 8, Table 1) and our previous investigation (Gutsmann et al., 1999) into changes of the innermembrane potential difference $\Delta\Phi$ of asymmetric bilayers. A decrease of $\Delta\Phi$ was observed, when the outer leaflet of the bilayer was composed of F515 LPS or R595 LPS, but an increase occurred in the case of R45 LPS (Table 1). The monolayer experiments, however, showed an increase of the surface potential after CAP18 intercalation for all three types of Re LPS (Fig. 8, Table 1). Considering the fact that $\Delta\Phi$ reflects a potential difference between the two monolayers of the bilayer and that CAP18 changes the potential of the different Re LPS monolayers in the same direction, the differences observed for the changes of $\Delta\Phi$ can only be explained by a different influence of CAP18 on the potential profile in the region of the PL leaflet. The different depth of CAP18 intercalation into the PL leaflet could either change the dipole potential or even the Gouy-Chapman potential on the PL leaflet if the molecule spans the complete bilayer.

The main differences of the three LPS used in our experiments are found in the headgroup region. One difference is found in the L-Ara*p*4N linked to position 2 of the reducing glucosamine of R595 LPS and R45 LPS. Another difference is the presence of a second in R45 LPS (Fig. 1). Resulting from this substitution the surface charge density of the three compounds is different (Table 1). The higher surface charge density of F515 LPS as compared to R45 LPS, however, only accounts for a slightly higher binding stoichiometry between CAP18 and F515 LPS. The observed differences in CAP18-induced membrane permeabilization (Gutsmann et al., 1999) are obviously due to the different depth of intercalation of the protein into the bilayer. A similar observation was made by Dathe et al. (1996) for different cationic model peptides. These authors found that a disturbance of the hydrophobic inner membrane region had a more dramatic effect on membrane permeability than accumulation of high peptide concentrations at the membrane surface. Regarding CAP18 resistance of *P. mirabilis*, the L-Ara*p*4N at position 2 of the reducing glucosamine of R45 LPS can not be the dominant structural component, because it is also present in the LPS of the CAP18 sensitive strain *Salmonella enterica* sv. Minnesota R595. Therefore, we propose that the L-Ara*p*4N $\beta(1\rightarrow8)$-linked to the first Kdo is responsible for CAP18-resistance by a steric hindrance causing a reduced depth of intercalation of CAP18 into the bilayer. Thus, we predict that neither electrostatic nor hydrophobic effects are responsible for the resistance against CAP18.

### Influence of Cations on the Interaction Between CAP18 and LPS Membranes

It has frequently been reported that cations — in particular divalent cations — protect bacteria against permeability-increasing effects of different peptides/proteins such as the bactericidal/permeability-increasing protein (BPI) and defensins (Selsted et al., 1985; Miyasaki et al., 1990; Wiese et al., 1997). In contrast to these observations, Mason et al. (1997) showed that the $CAP18_{106–137}$ activity did not depend on the concentration of $K^+$ (50 to 250 mM) and $Mg^{2+}$ (1 to 10 mM). Furthermore, it has been shown that $K^+$ (100 to 1000 mM) and $Mg^{2+}$ (0 to 5 mM) have no influence on the induction of lesions in reconstituted planar bilayers by CAP18 (Gutsmann et al., 1999).

$K^+$ and $Na^+$ had, however, an influence on the intercalation of CAP18 into F515 LPS liposomes, which became significant at concentrations >200 mM and caused a reduction by 40% at 1000 mM (Fig. 3*A*). At lower concentrations, $K^+$ and $Na^+$ in the absence or presence of 5 mM $Mg^{2+}$ had no influence (Fig. 3*B*). The CAP18 intercalation does not show a specificity for $K^+$ or $Na^+$, but is dependent on the ionic strength. From the reduced CAP18 binding capacity of Re LPS monolayers in the presence of 5 mM $Mg^{2+}$ (Fig. 6, Table 2), it can be deduced that the Gouy-Chapman potential is responsible for the binding stoichiometry between CAP18 and Re LPS. An increase in the area per CAP18 molecule, however, was only observed for R45 LPS monolayers (Table 2). Therefore, it can be concluded that only in the case of R45 LPS did $Mg^{2+}$ have an influence on the orientation of CAP18 molecules in the monolayers. At biologically relevant lateral pressures (25–30 $mN \cdot m^{-1}$), a concentration of 5 mM $MgCl_2$ in the subphase did not change the intercalation of rabbit CAP18 into the monolayers significantly (Fig. 5*A*, trace a, b). At higher lateral pressures, however, CAP18 or complexes of CAP18 and LPS were displaced from the monolayer. Furthermore, for $Mg^{2+}$ concentrations >5 mM intercalation of CAP18 into the monolayer was reduced (Fig. 5*A* and *B* trace c). These data clearly show an influence of $Mg^{2+}$ on the interaction of CAP18 with lipids, which could, however, not be observed by FRET spectroscopy or by electrophysiological measurements at planar bilayer membranes (Gutsmann et al., 1999), because in bilayer systems the lateral pressure does not exceed values of >30

$mN \cdot m^{-1}$ (Marcelja, 1974; Blume, 1979). Therefore, the influence of $Mg^{2+}$ is also not manifested in the biological activity of CAP18 against bacteria (Mason et al., 1997).

The smaller influence of divalent cations on the action of CAP18 in comparison to other cationic peptides/proteins can also be deduced from measurements of $Ca^{2+}$ displacement from Re LPS monolayers (Fig. 7). After addition of the polycationic CAP18 to the subphase, it accumulates at the negatively charged monolayer surface and displaces the $Ca^{2+}$ ions. This displacement is 18-fold higher than that by PMB (Fig. 8) and 3.4-fold higher than that by $rBPI_{21}$ (*data not shown*), which both are known to bind strongly to LPS (Srimal et al., 1996; Gazzano-Santoro et al., 1992). This and the fact that binding of CAP18 to negatively charged membranes is not as much reduced by divalent cations as that of other peptides/proteins, leads to the conclusion that the electrostatic interaction between CAP18 and Re LPS is not the sole force of interaction. This would be in accordance with the observation by Tossi et al. (1994) that a reduction of the number of positive charges in fragments of $CAP18_{106–125}$ has a smaller effect on the antibacterial activity than the change in its α-helical conformation or amphiphathicity.

### Change of Domain Structure in LPS Monolayers After CAP18 Addition

The epifluorescence micrographs showed a dramatic influence of CAP18 on the domain structure of endotoxin as shown for lipid A in Fig. 9 (changes in size and shape of the liquid condensed (LC) and liquid expanded (LE) domains). Furthermore, shortly after the addition of CAP18 a transient third domain type occurred (Fig. 9*B*) indicating that the protein intercalates preferentially into the boundary region between LC and LE domains. A similar observation was made by Ruano et al. (1998) for the intercalation of the pulmonary protein SP-A into dipalmitoylphosphatidylcholine and DPPC/dipalmitoylphosphatidyl-glycerol monolayers. It can, however, not be definitely decided, whether incorporation of CAP18 provokes a dissolution of the LC domains or the formation of a larger number of smaller LC domains below the resolution of the optical setup (~1 μm). The observation of a higher fluorescence intensity in the LE domains prior to addition of CAP18 is in favor of the latter possibility (Fig. 9*B* and *C*). The changes in the domain structure of Re LPS and lipid A monolayers induced by CAP18 could result from (i) a fluidization of the acyl chains (decrease of $T_c$) of LPS or (ii) a CAP18-induced reduction of the cooperativity of LPS molecules leading to the dissolution of the domains or the formation of microdomains of CAP18 oligo- or multimers. The FTIR data, however, gave no evidence of an influence of CAP18 on the phase transition temperature $T_c$ (Fig. 11). Thus, one of the latter interaction mechanisms is more likely.

### Influence of LPS on Secondary Structure of CAP18

The α-helical structure of CAP18 is enhanced in the presence of Re LPS (Fig. 10). This implies that binding of CAP18 to Re LPS leads to an increased order of the protein in the membrane. This finding is in excellent agreement with those of Chen et al. (1995), who found in experiments using circular dichroism an increase of the formation of helical structure following binding of the active CAP18 fragment $CAP18_{106–137}$ to lipid A. Also for a number of other cationic antibacterial peptides/proteins like indolicidin (Falla, Karunaratne & Hancock, 1996) and magainin (Matsuzaki et al., 1991), the α-helical structure becomes more pronounced upon interaction with negatively charged lipids.

In summary, our data show that a basic requirement for the interaction of rabbit CAP18 with lipid membranes is a negatively charged lipid (step (i) of the model of CAP18 action). Furthermore, the chemical structure of the inner core region of the LPS, in particular the presence of substituents plays a major role for an understanding of the different sensitivity of various Gram-negative strains to CAP18. Step (ii) of our proposed model could now be identified to be the critical step for sensitivity or resistance. The type of Re LPS governs the depth of intercalation of the protein into the membrane and it is, with that, decisive for the resistance/sensitivity of the respective bacterial strain towards CAP18. In particular in the case of *P. mirabilis*, the additional L-Ara*p*4N β(1→8)-linked to the first Kdo is the structural component being responsible for the resistance of these bacteria. In the following step (iii) the depth of intercalation of CAP18 into the membrane is inversely proportional to the amplitude of the clamp-voltage required for the induction of membrane lesions (Gutsmann et al., 1999). Finally, for the design of new antibacterial therapeutics based on CAP18, we predict that a prerequisite for high efficacy will be a deep intercalation of the peptide into the bacterial outer membrane.

We are indebted to Mr. D. Koch for performing some of the film balance measurements, to Mrs. A.B. Schromm and Mrs. C. Hamann for the FRET measurements, to Mr. K. Brandenburg and Mr. G. von Busse for the FTIR measurements, and to Mr. U. Seydel for his insightful comments and critical reading of the manuscript. This work was financially supported by the Deutsche Forschungsgemeinschaft (Grants SFB 470, Project B5 and Br 1070/2-1) and the Federal Ministry of Education, Science, Research, and Technology (BMBF Grant 01 KI 9851, Project A6). T.G. acknowledges a fellowship of the Sparkassenstiftung Schleswig-Holstein.

## References


Arrondo, J.L.R., Muga, A., Castresana, J., Goni, F.M. 1993. Quantitative studies of the structure of proteins in solution by Fourier-transform infrared spectroscopy. *Prog. Biophys. Mol. Biol.* **59:**23–56

Bals, R., Weiner, D.J., Meegalla, R.L., Wilson, J.M. 1999. Transfer of a cathelicidin peptide antibiotic gene restores bacterial killing in a cystic fibrosis xenograft model. *J. Clin. Invest.* **103:**1113–1117

Bechinger, B., Zasloff, K., Opella S.J. 1993. Structure and orientation of the antibiotic peptide magainin in membranes by solid-state nuclear magnetic resonance spectroscopy. *Protein Sci.* **2:**2077–2084

Blume, A. 1979. A comparative study of the phase transitions of phospholipid bilayers and monolayers. *Biochim. Biophys. Acta* **557:**32–44

Brandenburg, K., Kusumoto, S., Seydel, U. 1997. Conformational studies of synthetic lipid A analogues and partial structures by infrared spectroscopy. *Biochim. Biophys. Acta* **1329:**183–201

Brockman, H. 1994. Dipole potential of lipid membranes. *Chem. Phys. Lipids* **73:**57–79

Chen, C., Brock, R., Luh, F., Chou, P.-J., Larrick, J.W., Huang, R.-F., Huang, T.-H. 1995. The solution structure of the active domain of CAP18-a lipopolysaccharide binding protein from rabbit leukocytes. *FEBS Lett.* **370:**46–52

Cowland, J.B., Johsen, A.H., Borregaard, N. 1995. hCAP-18, a cathelin/pro-bactenecin-like protein of human neutrophil specific granules. *FEBS Lett.* **368:**173–176

Dathe, M., Schümann, M., Wieprecht, T., Winkler, A., Beyermann, M., Krause, E., Matsuzaki, K., Murase, O., Bienert, M. 1996. Peptide helicity and membrane surface charge modulate the balance of electrostatic and hydrophobic interactions with lipid bilayers and biological membranes. *Biochemistry* **35:**12612–12622

Falla, J.T., Karunaratne, D.N., Hancock, R.E.W. 1996. Mode of action of the antimicrobial peptide indolicidin. *J. Biol. Chem.* **271:**19298–19303

Fringeli, U.P., Günthard, H.H. 1981. Infrared membrane spectroscopy. *In:* Membrane Spectroscopy (E. Grell, Editor) Springer-Verlag, Berlin

Galanos, C., Lüderitz, O., Westphal, O. 1969. A new method for the extraction of R lipopolysaccharides. *Eur. J. Biochem.* **9:**245–249

Gazzano-Santoro, H., Parent, J.B., Grinna, L., Horwitz, A., Parsons, T., Theofan, G., Elsbach, P., Weiss, J., Conlon, P.J. 1992. High-affinity binding of the bactericidal/permeability-increasing protein and a recombinant amino-terminal fragment to the lipid A region of lipopolysaccharide. *Infect Immun.* **60:**4754–61

Gutsmann, T., Larrick, J.W., Seydel, U., Wiese, A. 1999. Molecular mechanisms of interaction of rabbit CAP18 with outer membranes of Gram-negative bacteria. *Biochemistry* **38:**13643–13653

Hancock, R.E.W. 1984. Alterations in outer membrane permeability. *Ann. Rev. Microbiol.* **38:**237–264

Hirata, M., Shimomura, Y., Yoshida, M., Wright, S.C., Larrick, J.W. 1994. Endotoxin-binding synthetic peptides with endotoxin-neutralizing, antibacterial and anticoagulant activities. *Prog. Clin. Biol. Res.* **388:**147–159

Hirata, M., Zhong, J., Wright, S.C., Larrick, J.W. 1995. Structure and functions of endotoxin-binding peptides derived from CAP18. *Prog. Clin. Biol. Res.* **392:**317–326

Kauppinen, J.K., Moffat, D.J., Mantsch, H.H., Cameron, D.G. 1981. Fourier self-deconvolution: a method for resolving intrinsically overlapped bands. *Appl. Spectrosc.* **35:**271–276

Larrick, J.W., Hirata, M., Shimomoura, Y., Yoshida, M., Zheng, H., Zhong, J., Wright, S.C. 1993. Antimicrobial activity of rabbit CAP18-derived peptides. *Antimicrob. Agents Chemother.* **37:**2534–2539

Larrick, J.W., Hirata, M., Zheng, H., Zhong, J., Bolin, D., Cavaillon, J.-M., Warren, H.S., Wright, S.C. 1994. A novel granulocyte-derived peptide with lipopolysaccharide-neutralizing activity. *J. Immunol.* **152:**231–240

Larrick, J.W., Morgan, J.G., Palings, I., Hirata, M., Yen, M.H. 1991. Complementary DNA sequence of rabbit CAP18—a unique lipopolysaccharide binding protein. *Biochem. Biophys. Res. Commun.* **179:**170–175

Lüllmann, H., Plösch, H., Ziegler, A. 1980. Ca replacement by cationic amphiphilic drugs from lipid monolayers. *Biochem. Pharmacol.* **29:**2969–2974

Mantsch, S., McElhaney, R.N. 1991. Phospholipid phase transitions in model and biological membranes as studied by infrared spectroscopy. *Chem. Phys. Lipids* **57:**213–226

Marcelja, S. 1974. Chain ordering in liquid crystals. II. Structure of bilayer membranes. *Biochim. Biophys. Acta* **367:**165–176

Mason, D.J., Dybowski, R., Larrick, J.W., Gant, V.A. 1997. Antimicrobial action of rabbit leukocyte CAP18(106-137). *Antimicrob. Agents Chemother.* **41:**624–629

Matsuzaki, K. 1998. Magainins as paradigm for the mode of action of pore forming polypeptides. *Biochim. Biophys. Acta* **1376:**391–400

Matsuzaki, K., Haradar, M., Handa, T., Funakoshi, S., Fujii, N., Yajima, H., Miyajima, K. 1991. Physicochemical determinants for the interactions of magainins 1 and 2 with acidic lipid bilayers. *Biochim. Biophys. Acta* **1063:**162–170

Miyasaki, K.T., Bodeau, L., Ganz, T., Selsted, M.E., Lehrer, R.I. 1990. In vitro sensitivity of oral, gram-negative, facultative bacteria to the bactericidal activity of human neutrophil defensins. *Infect. Immun.* **58:**3934–3940

Pickard, W.F., Sehgal, K.C., Jackson, C.M. 1979. Measurement of phospholipid monolayer surface potentials at a hydrocarbon-electrolyte interface. *Biochim. Biophys. Acta* **552:**1–10

Rietschel, E.T., Brade, L., Lindner, B., Zähringer, U. 1992. Biochemistry of lipopolysaccharides. *In:* Bacterial Endotoxic Lipopolysaccharides, Vol. I: Molecular biochemistry and cellular biology (D.C. Morrison and J.L. Ryan, Editors) pp. 3–41. CRC Press, Boca Raton, FL

Rietschel, E.T., Kirikae, T., Schade, F.U., Mamat, U., Schmidt, G., Loppnow, H., Ulmer, A.J., Zähringer, U., Seydel, U., Di Padova, F., Schreier, M., Brade, H. 1994. Bacterial endotoxin: molecular relationships of structure to activity and function. *FASEB J.* **8:**217–225

Ruano, M.L.F., Nag, K., Worthman, L.-A., Casals, C., Perez-Gil, J., Keough, K.M.W. 1998. Differential partitioning of pulmonary surfactant protein SP-A into regions of monolayers of dipalmitoylphosphatidylcholine and dipalmitoylphosphatidylcholine/dipalmitoylphosphatidylglycerol. *Biophys. J.* **74:**1101–1109

Schromm, A.B., Brandenburg, K., Loppnow, H., Zähringer, U., Rietschel, E.T., Carroll, S.F., Koch, M.H.J., Kusumoto, S., Seydel, U. 1998. The charge of endotoxin molecules influences their conformation and IL-6-inducing capacity. *J. Immunol.* **161:**5464–71

Schumann, D. 1989. Electrical properties of adsorbt or spread films: the effective value of permittivities in the Helmholtz equation. *J. Colloid Interface Sci.* **134:**152–160

Schwarz, G., Taylor, S.E. 1995. Thermodynamic analysis of the surface activity exhibited by a largely hydrophobic peptide. *Langmuir* **11:**4341–4346

Selsted, M.E., Szklarek, D., Ganz, T., Lehrer, R.I. 1985. Activity of rabbit leukocyte peptides against *Candida albicans*. *Infect. Immun.* **49:**202–206

Struck, D.K., Hoekstra, D., Pagano, R.E. 1981. Use of resonance energy transfer to monitor membrane fusion. *Biochemistry* **20:**4093–4099

Srimal, S., Surolia, N., Balasubramanian, S., Surolia, A. 1996. Titration calorimetric studies to elucidate the specificity of the interactions of polymyxin B with lipopolysaccharides and lipid A. *Biochem. J.* **315:**679–686

Tossi, A., Scocchi, M., Skerlavaj, B., Gennaro, R. 1994. Identification and characterization of a primary antibacterial domain in CAP18, a lipopolysaccharide binding protein from rabbit leukocytes. *FEBS Lett.* **339:**108–112

Viljanen, P., Koski, P., Vaara, M. 1988. Effect of small cationic leukocyte peptides (defensins) on the permeability barrier of the outer membrane. *Infect. Immun.* **56:**2324–2329

Vinogradov, E.V., Thomas-Oates, J.E., Brade, H., Holst, O. 1994. Structural investigation of the lipopolysaccharide from *Proteus mirabilis* R45 (Re-chemotype). *J. Endotoxin Res.* **1:**199–206

Vogel, V., Möbius, D. 1988. Local surface potentials and electric dipole moments of lipid monolayers: contributions of the water/lipid and lipid/air interface. *J. Colloid Interface Sci.* **126:**408–420

von Tscharner, V., McConnell, H.M. 1981. An alternative view of phospholipid phase behavior at the air-water interface. Microscope and film balance studies. *Biophys. J.* **36:**409–419

Weis, R.M. 1991. Fluorescence microscopy of phospholipid monolayer phase transitions. *Chem. Phys. Lipids* **57:**227–239

Wiese, A., Brandenburg, K., Carroll, S.F., Rietschel, E.Th., Seydel, U. 1997. Mechanisms of action of bactericidal/permeability-increasing protein BPI on reconstituted outer membranes of Gram-negative bacteria. *Biochemistry* **36:**10311–10319

Wiese, A., Brandenburg, K., Lindner, B., Schromm, A.B., Carroll, S.F., Rietschel, E.Th., Seydel, U. 1997. Mechanisms of action of the bactericidal/permeability-increasing protein BPI on endotoxin and phospholipid monolayers and aggregates. *Biochemistry* **36:**10301–10310

Wiese, A., Münstermann, M., Gutsmann, T., Lindner, B., Kawahara, K., Zähringer, U., Seydel, U. 1998. Molecular mechanisms of polymyxin B-membrane interactions: direct correlation between surface charge density and self-promoted transport. *J. Membrane Biol.* **162:**127–138

Zähringer, U., Lindner, B., Seydel, U., Rietschel, E.T., Naoki, H., Unger, F.M., Imoto, M., Kusumoto, S., Shiba, T. 1985. Structure of de-O-acylated lipopolysaccharide from *Escherichia coli* Remutant strain F515. *Tetrahedron Lett.* **26:**6321–6324